

RESEARCH

Open Access



PRP significantly promotes the adhesion and migration of vascular smooth muscle cells on stent material

Yin-Di Wu^{1,2}, Hong-Jing Jiang^{1,2}, Hao-Hao Zhou³, Jian-Yi Xu¹, Qing Liu⁴, Xu-Heng Sun¹, Yue-Heng Wu² and Zhan-Yi Lin^{1,2*}

Abstract

Background The adhesion and survival state of cells on scaffold material is a major problem in tissue-engineered blood vessel (TEBV) culture. Platelet-rich plasma (PRP) contains a large amount of biologically active factors and fibrin, which is expected to play an important role in TEBV culture.

Purpose To combine PRP with cells and scaffold material to promote cell adhesion and biological activity on the scaffold material.

Methods The adhesion status and migration of SMCs under the optimal concentration suitable for SMC growth and the optimal concentration of PRP were examined by scanning electron microscopy, HE staining, CCK-8 assays, qPCR, WB, and other experimental methods and compared with those under the conventional culture (20% FBS); finally, the effect of PRP on the deposition of ECM in vascular tissue engineering culture was verified by three-dimensional culture.

Results PRP at 20% is a suitable concentration for SMCs. Compared with the control group, the 20% PRP group had better migration, and the number of SMC adhesions was significantly higher than that of the control group. In addition, collagen deposition in the experimental group was significantly higher than that in the control group.

Conclusion PRP (20%) can promote SMC adhesion, migration, and collagen deposition on the scaffold material.

Keywords Platelet-rich plasma (PRP), Smooth muscle cell (SMC), Cell migration assays, Decellularized extracellular matrix (ECM)

Introduction

The culture of tissue-engineered blood vessels consists of three basic elements: an adequate amount of seed cells, a suitable scaffold material, and a complex culture environment [1, 2]. Due to the long culture time, the adhesion status of seed cells on top of the scaffold material is directly related to the outcome of TEBV culture. PGA material is a biodegradable polymer hydrophobic material that can develop a porous three-dimensional structure through nonwoven technology [3]. We found that in the traditional method for TEBV culture, adhesion of smooth muscle cells on

*Correspondence:

Zhan-Yi Lin

linzhanyi@gdph.org.cn

¹ School of Medicine, South China University of Technology, Guangzhou 510006, Guangdong, China

² Guangdong Provincial People's Hospital (Guangdong Academy of Medical Sciences, Guangdong Academy of Medical Sciences), South Medical University, Guangzhou 510080, Guangdong, China

³ Ji Hua Institute of Biomedical Engineering Technology, Ji Hua Laboratory, Foshan 528200, Guangdong, China

⁴ School of Biological Sciences and Engineering, South China University of Technology, Guangzhou 510006, Guangdong, China



© The Author(s) 2023. **Open Access** This article is licensed under a Creative Commons Attribution 4.0 International License, which permits use, sharing, adaptation, distribution and reproduction in any medium or format, as long as you give appropriate credit to the original author(s) and the source, provide a link to the Creative Commons licence, and indicate if changes were made. The images or other third party material in this article are included in the article's Creative Commons licence, unless indicated otherwise in a credit line to the material. If material is not included in the article's Creative Commons licence and your intended use is not permitted by statutory regulation or exceeds the permitted use, you will need to obtain permission directly from the copyright holder. To view a copy of this licence, visit <http://creativecommons.org/licenses/by/4.0/>. The Creative Commons Public Domain Dedication waiver (<http://creativecommons.org/publicdomain/zero/1.0/>) applies to the data made available in this article, unless otherwise stated in a credit line to the data.

the nonwoven PGA material adhesion is poor, cells in an uncontrollable proportion fall on the bottom of the reactor or fall on the bottom of the current technology and cannot be completely removed, and part of the residual seed cells will be in the bottom and cocultured with TEBVs. On the one hand, the cells will remove the upper part of the TEBV nutrients. On the other hand, the bottom cells die when they reach a certain density, and it is not known whether some factors will be released in this process to have uncontrollable effects on the upper TEBV layer.

To make the culture process smoother and to improve the biological activity of seeded cells on the scaffold material, many scholars have tried various methods [4], and some scholars combined gelatin and PLLA material and found that it could improve cell adhesion and migration on the material. LI electrospun keratin and PCL material were used to form a composite vascular tissue engineering scaffold material, and this biocomposite scaffold enhanced endothelial cell (EC) adhesion and growth [5]. Some researchers have also enhanced cell adhesion on top of the material by adding collagen or both fibrin and gelatin [6, 7]. These methods modify the properties of the material by altering its surface morphology and characteristics, but the techniques are more complex.

Growth factors play an important role in biological activities, such as cell adhesion, migration, secretion, and proliferation [8, 9]. Platelet-rich plasma (PRP) contains a variety of growth factor components, such as TGF, VEGF, and PDGF. PRP also contains fibronectin, a three-dimensional meshwork structure that can effectively store a variety of growth factors and cells [10]. PRP is widely available, easy to obtain, and commercially available. It can be obtained repeatedly and multiple times with minimal trauma [11–13] and is already available in established commercial products. We promoted the adhesion and migration of SMCs on top of the scaffold material by adding a certain concentration of PRP to the smooth muscle cell suspension and then placing it onto the PGA scaffold.

Materials and methods

All experiments were conducted in accordance with the ethical regulations of Guangdong Provincial People's Hospital, Guangdong Academy of Medical Sciences, and the ethics number is No. GDREC2019285h (RI).

Nonwoven PGA material was purchased from the United States (Biomedical Structures, Rhode Island, Warwick, USA), PRP was obtained from six healthy volunteers (aged 25–31 years), all with informed signed consent, and smooth muscle cells were obtained from the residual human aortic tissue of a heart transplant donor.

Preparation of PRP

The two-step centrifugation method was used to obtain PRP. First, venous blood was taken with anticoagulation tubes containing sodium citrate (KWS, China), and two-step centrifugation was performed at 200 g*15 min and 400 g*15 min to collect PRP and PPP components. Whole blood and PRP were subjected to platelet counting, so that the platelet concentration of PRP was four-to-six times that of whole blood [14, 15]. Platelet markers were stained using the Richter (Biosharp, China) staining method. The PRP was stored at – 80 °C for 1 h and then thawed at room temperature for 1 h. The procedure was repeated three times, and the PRP solution without cells was obtained by centrifugation for the following experiments and stored at – 80 °C [15].

Isolation and identification of SMCs

Human aortic tissue samples of 2 cm*2 cm were used for primary culture of smooth muscle cells by the appanation culture method. Briefly, the mesangial tissues were first evenly attached to a T25 culture flask (Corning, USA) and incubated in a 37 °C incubator (Thermo, USA) containing 5% CO₂, and 4–5 ml of DMEM/F12 (Dulbecco's Modified Eagle Medium, Corning, USA) medium containing 20% FBS (Fetal Bovine Serum, Gibco, USA) was added [16]. After 4 h, the flask was not shaken for 1 week to prevent the tissue from floating and the cells from climbing out. After 2 weeks, the cells were passaged until the P3 generation, 5*10⁴ cells were collected on cell crawlers (Biosharp, China), immunofluorescence staining was performed according to the instructions, and the cells were treated with antibody (calponin, smoothelin, 1:500, Abcam, USA) and DAPI working solution (Solarbio, China). Then, the samples were processed and examined microscopically [17].

Electron microscopic detection

PGA materials from different treatment groups (A: control group treated with 20% FBS, B: experimental group treated with 20% PRP, C: control group with smooth muscle cells, and D: experimental group with smooth muscle cells) were fixed with 3 ml of 2.5% glutaraldehyde, the samples were rinsed in 0.1 mol/L sodium dimethylcarbamate buffer (pH 7.4), and the PGA materials were placed in buffer solution at 4 °C overnight. Twenty-four hours later, the buffer solution was removed, and the PGA materials were soaked in 1% citric acid for 1 h. The PGA materials were repeatedly rinsed with the buffer solution. After that, the PGA material was subjected to gradient dehydration

treatment and finally treated with isoamyl acetate alternate. Observations were performed with a scanning electron microscope (S-3500N, Japan) [18].

Growth factor release assay

To determine the ability and time of PRP to release growth factors on top of PGA material, we used PDGF and TGF- β 1 as assay indicators. The above nonwoven PGA material was used at 1 cm*1 cm, and PRP was pre-configured into 20% PRP solution with DMEM/F12. One hundred microliters of 20% PRP solution was taken and injected dropwise onto the PGA material, fixed with a cotton swab, and placed in a 24-well plate (Corning, USA) for incubation, and 1 ml of PBS solution was added to each well. The medium was collected at different time points and placed at -80°C . The medium was stored at -80°C for 3, 6, 9, 12, 15, 18, 21, 24, 27, and 30 days according to the instructions (DuoSet[®]; R&D Systems, Minneapolis, MN, USA), and the concentrations of PDGF and TGF- β 1 released from the assay material were quantified by ELISAs.

CCK-8 experiment

SMCs in different groups (20% FBS, 10% PRP, 20% PRP, 30% PRP, 40% PRP, 50% PRP, and 100% PRP) were inoculated in 96-well plates ($n=6$) at a density of 3000 cells/well for 1, 3, 5, 7, and 9 days, and 10% CCK-8 reagent was added according to the CCK-8 kit (Dojindo, Japan) and incubated for 2 h at 37°C . Then, the absorbance of the medium at 450 nm was measured by enzyme marker and compared [19].

Cell scratch experiments

SMCs in different groups (20% FBS, 20% PRP) were plated in 6-well plates at 10^4 cells/well ($n=6$), and the cells were laterally scored in the middle of the well plate with a 20 μl gun tip and photographed at 0–6–12–18 h. The scored area was calculated using ImageJ [20].

Quantitative real-time PCR

SMCs in different groups (20% FBS, 20% PRP) were plated in 6-well plates at 10^4 cells/well ($n=3$) and incubated in DMEM with 20% FBS for 3 days. Then, total RNA was extracted using the TRIzol kit (TaKaRa, Japan) according to the instructions, total RNA was reverse transcribed using the reverse transcription kit (TaKaRa, Japan), and the cDNA obtained by reverse transcription was used with SYBR Premix Ex Taq (TaKaRa, Japan) according to the instructions [11]. The conditions for real-time PCR were 40 cycles at 95°C for 10 s and 60°C for 30 s, and GAPDH was used as a reference. The following is the base pair composition of the primers used (Table 1):

Table 1 Real-time PCR primers and product sizes

Gene		Sequence (5'-3')	Size (bp)
GSK3B	Sense	TATGGCTGCTGGCTGTGTG	120
	Antisense	GCTCCCTTGTGGAGTCCC	
CTNNB1	Sense	GTACCGGAGCCCTTCACATC	165
	Antisense	CAGCTTCCTGTCTGAGCA	
MMP2	Sense	AGGATGGCAAGTACGGCTTC	185
	Antisense	CTTCTGTGCGGTCTGTAGT	
MMP9	Sense	GGACAAGCTCTCGGCTTCT	126
	Antisense	TCGCTGGTACAGTTCGAGTA	
GAPDH	Sense	TTCGTCATGGGTGTGAACCA	170
	Antisense	GTCTTCTGGGTGGCAGTGAT	

Western blot (WB) experiment

SMC processing was performed as above. Prior to the start of the WB experiments, proteins were lysed using a protein extraction kit containing protease inhibitors and RIPA (Solarbio, China), and the concentration of total protein was detected using a BCA kit (Biosharp, China) according to the kit's instructions [21]. The spiked volume was calculated in advance, the samples were added to 12% SDS polyacrylamide gels, keeping the concentration of the spiked samples consistent, and the total volume of the spiked samples did not exceed 25 μl . Electrophoresis was performed at a voltage of 100–120 V for 40–60 min, followed by removal of the upper part of the dentate gel and the lower part of the excess gel components, and the gel was transferred to a polyvinylidene difluoride membrane (Millipore) at 140–160 V for 30 min, followed by incubation in 5% skim milk in Tris-buffered saline containing 0.05% and 1% Tween 20 (TBST) for blocking. Then, the membrane was incubated with the following primary antibodies: anti-CNN (1:500; Abcam, USA), anti-SMTN (1:2000; Abcam, USA), anti-GSK-3 β (1:1000; Abcam, USA), anti-p-GSK-3 β (1:500; Abcam, USA), anti-catenin (1:500; Abcam, USA), anti-COL I (1:1000; Abcam, USA), anti-MMP2 (1:500; Abcam, USA), anti-GAPDH (1:10,000; Abcam, USA), and anti-Histone (1:10,000; Abcam, USA). Finally, the Millipore membrane was subjected to chemiluminescence detection using ECL protein blotting substrate (Pierce). Chemiluminescence detection was performed, followed by development of the film using an exposure machine (Tanon, Shanghai, China).

Three-dimensional culture and Masson staining experiments

The PGA material was processed into 1 cm*1.95 cm squares, soaked in 1 M NaOH solution alkaline for

1 min, and rinsed in sterile water three times for 5 min each time. Then, the PGA material was sutured on wooden sticks containing silicone tubes with 6-0 sterile sutures and sterilized by ethylene oxide, and cell inoculation was performed on the PGA material the next day [22], with a cell density of 1×10^7 cells/ml. The assembled material was cultured in DMEM/F12 containing 20% fetal bovine serum for 4 weeks, and the vascular matrix material was removed after 4 weeks for WB experiments and Masson staining [23]. Masson trichrome staining was performed according to the instructions (PhyEasy, China) and can be briefly summarized as sectioning, dewaxing, Masson trichrome staining, dehydration, transparency, and sealing. Collagen was stained blue.

Statistical analysis

All reported values were averaged ($n=6$) and are expressed as the mean \pm standard deviation (SD), and significant differences were determined with a two-sample t test assuming equal variances. A value of $p < 0.05$ was considered statistically significant.

Results

Fig. 1 A shows a schematic diagram of the production and application of PRP. A large number of platelet particles stained blue were observed on the PRP smear by Richter’s staining (Fig. 1 B, C). By selecting five different fields of view for platelet counting, we found that the number of PRP platelets was 4.96 times higher than that of whole blood (Fig. 1 D), which was consistent with the preparation criteria of PRP

The optimal concentration of PRP for use was tested by a CCK-8 assay, and smooth muscle cell phenotypes were identified in cells from the control and experimental groups. Calponin and smoothelin are markers of contractile phenotypes of smooth muscle cells, and the phenotypic expression of both types in smooth muscle cells was found to be close to 100% by immunofluorescence analysis (Fig. 2A–G). The CCK-8 results showed that 20%, 30%, and 40% PRP all had a pro-proliferative effect on SMCs, with the 20% PRP group showing the most prominent pro-proliferative effect, and the differences were significantly different at days 5, 7, 9, and 11 (Fig. 2J). Therefore, subsequent experiments were conducted using 20% PRP for the experimental group and 20% FBS for the control group for subsequent experimental studies. WB experiments revealed that the cells used in both

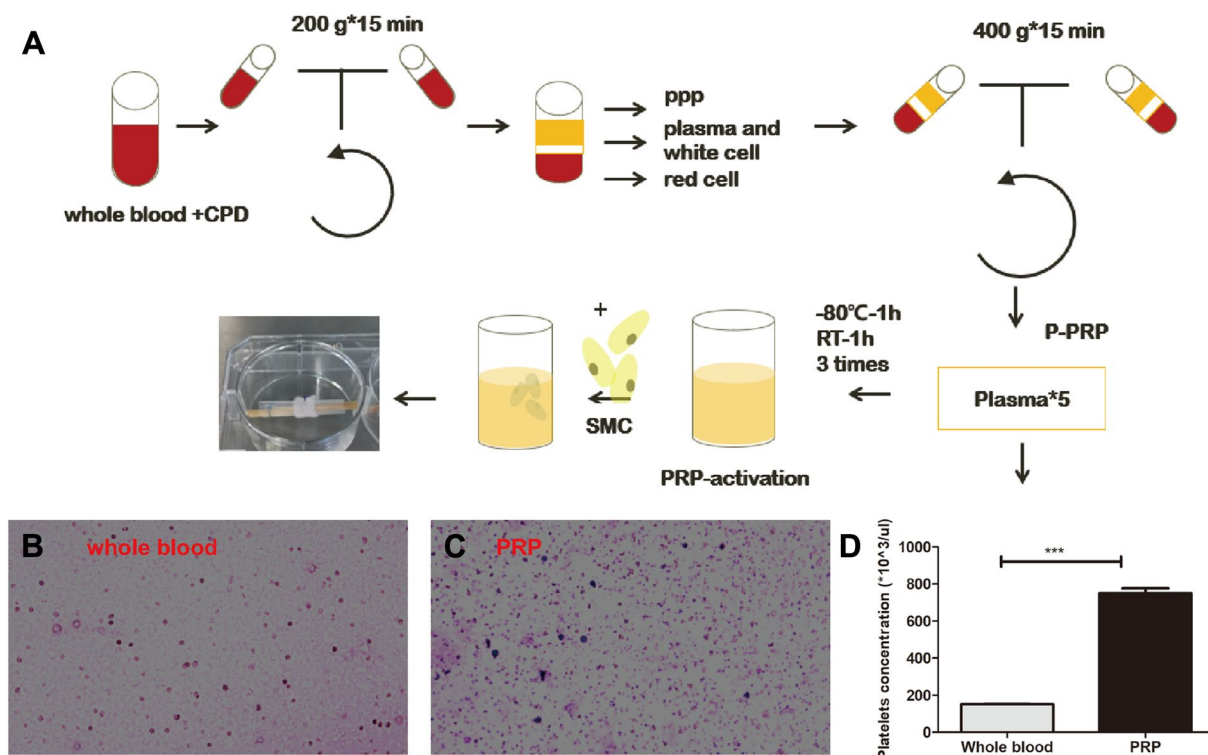


Fig. 1 Schematic diagram of the process of PRP treatment and application, diagram of the process of PRP from treatment to use (A), graphs of Richter staining of whole blood and PRP (B, C), bar graphs of platelet count statistics (D), and comparison with the blank group *** $p < 0.001$. All scale bars = 50 μ m

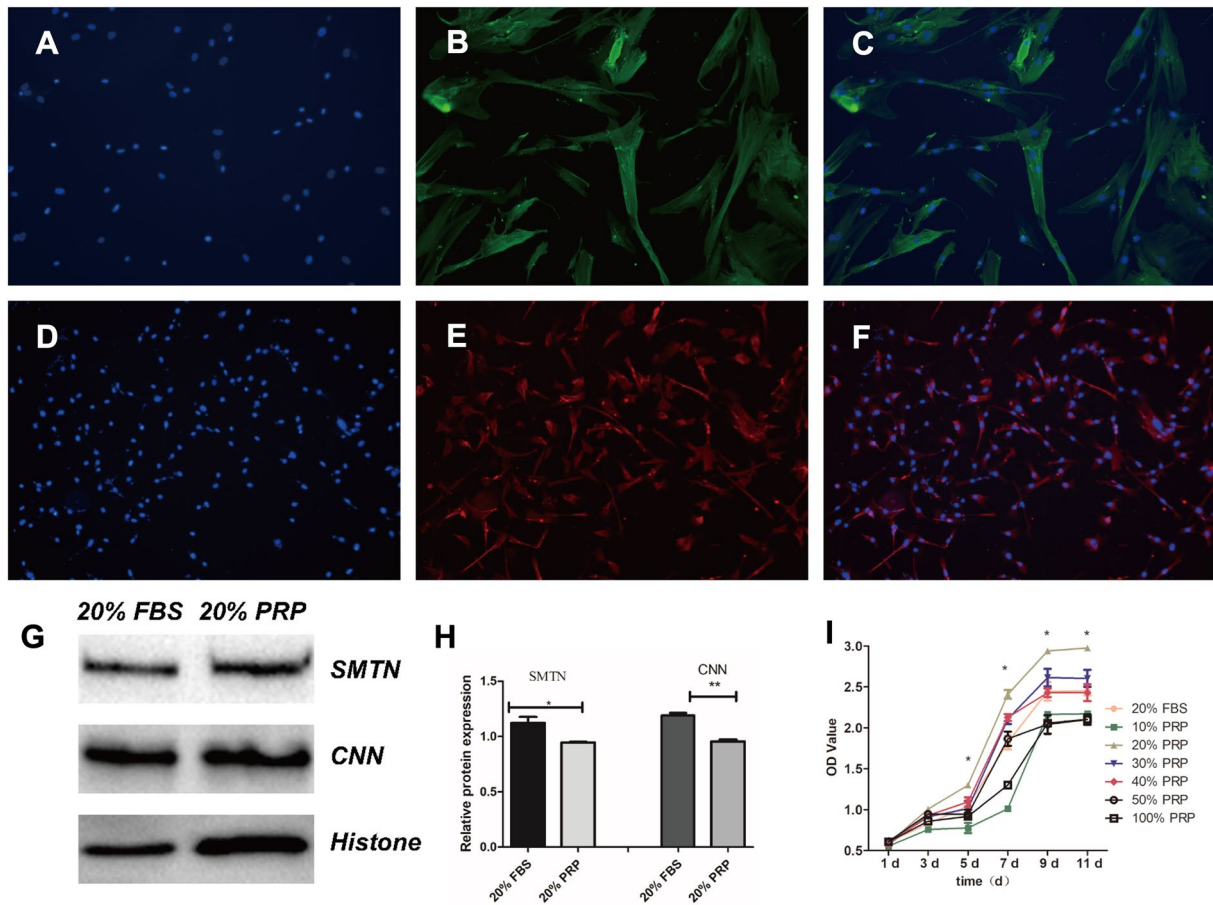


Fig. 2 Graphs of cell phenotypic identification and results of CCK-8 experiments and graphs of cellular immunofluorescence results in the control and experimental groups (A–F). Graphs of calponin and smoothelin WB assays and their grayscale value measurements. **G, H** Graphs of the effect of different PRP concentrations on the proliferative activity of smooth muscle cells by CCK-8 assays (**I**). * $p < 0.05$, ** $p < 0.01$, *** $p < 0.001$ compared to the blank group. All scale bars = 50 μm

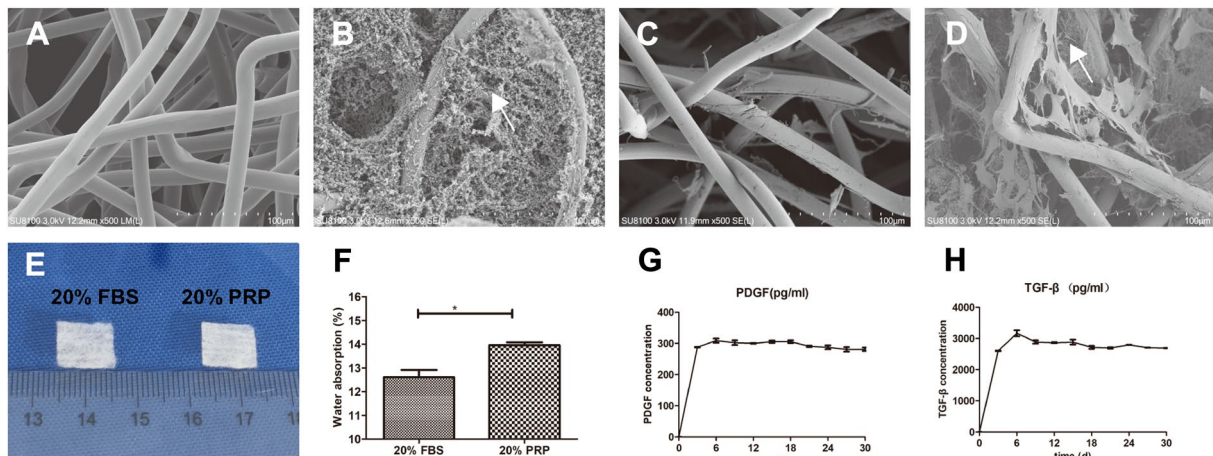


Fig. 3 Electron microscopic detection plots, bulk plots, and growth factor release curves over time for PGA materials in the control and experimental groups. Electron micrographs of different PGA treatments (A, B), electron micrographs of cells treated with different PGA treatments (C, D), PDGF, and TGF- β after PRP treatment with PGA material for 1 month [release graphs (G, H)]. \rightarrow Indicates the location of fibrin, * $p < 0.05$ compared to the blank group, *** $p < 0.001$. All scale bars = 100 μm

the experimental and control groups expressed the calponin and smoothelin proteins (Fig. 2H, I).

Electron microscopy showed that the PGA material in the PRP group contains a large number of loose fibrin filaments in the middle, as shown by the arrows, compared with that of the control group (Fig. 3B). The cells in the control group adhered to the PGA scaffold, the PGA gap was due to the large pores, a small number of cells attached to the PGA filaments, the cells attached to the PGA filaments had a single morphology, and fewer tentacles were tightly attached to the PGA filaments. In general, the number of smooth muscle cells visible in the field of view was significantly less than that of the experimental group (Fig. 3A, C), and in the experimental group, due to the presence of fibronectin, smooth muscle cells could be seen in addition to the PGA filaments, and smooth muscle cells were also observed between the PGA pores attached to fibronectin, with a variety of cell morphologies and wide tentacles (Fig. 3D). Figure 3E shows a general view of PGA, which is usually a multihollow mesh structure; the water absorption of the two materials was measured, and the PRP group showed significantly more absorption than the control group (Fig. 3F). The release of growth factors was found to be sustained for one month after PRP treatment (Fig. 3G, H).

The results of cell adhesion experiments showed that the PGA material treated with PRP had better adsorption to smooth muscle cells, and the observation of dropped cells at the bottom after inoculation and resting revealed that the control group had more dropped cells at the bottom, reaching 5% of the inoculation number, while almost no dropped cells were observed at the bottom of

the experimental group (Fig. 4A–C). The contents of the genes CTNNB1 and GSK3β and their regulatory proteins GSK-3β and β-catenin were detected by qPCR and WB analyses, and it was found that the gene expression was upregulated in the experimental group, and the protein content of both P-GSK-3β and β-catenin increased. The results indicated that PRP also promoted the protein expression of GSK-3β-activated β-catenin by upregulating adhesion-related genes, thereby promoting cell adhesion (Fig. 4D–F).

The results of the cell scratch assay showed that there was no significant difference in the cell migration rate between the experimental and control groups at hour 4. At hour 8, the cell migration rate was faster in the PRP group, and the difference was statistically significant (Fig. 5A–K). qPCR showed that the cell migration-related genes MMP-2 and MMP-9 were both upregulated in the experimental group versus the control group (Fig. 5L, M). There was no difference in the expression of MMP2 protein (Fig. 5N, O).

The cells of the experimental group and the control group were placed in 6-well plates for three-dimensional culture (Fig. 6A), and the cultures were removed after 4 weeks of static culture. The cultures were subjected to Masson staining and WB analysis of collagen content, and the results of Masson staining showed that the cells of the experimental group were more closely arranged, the collagen was stained blue, and the blue-stained collagen content of the experimental group was significantly higher than that of the control group, as seen by the naked eye. ImageJ statistics also confirmed this pattern, and the difference was statistically significant

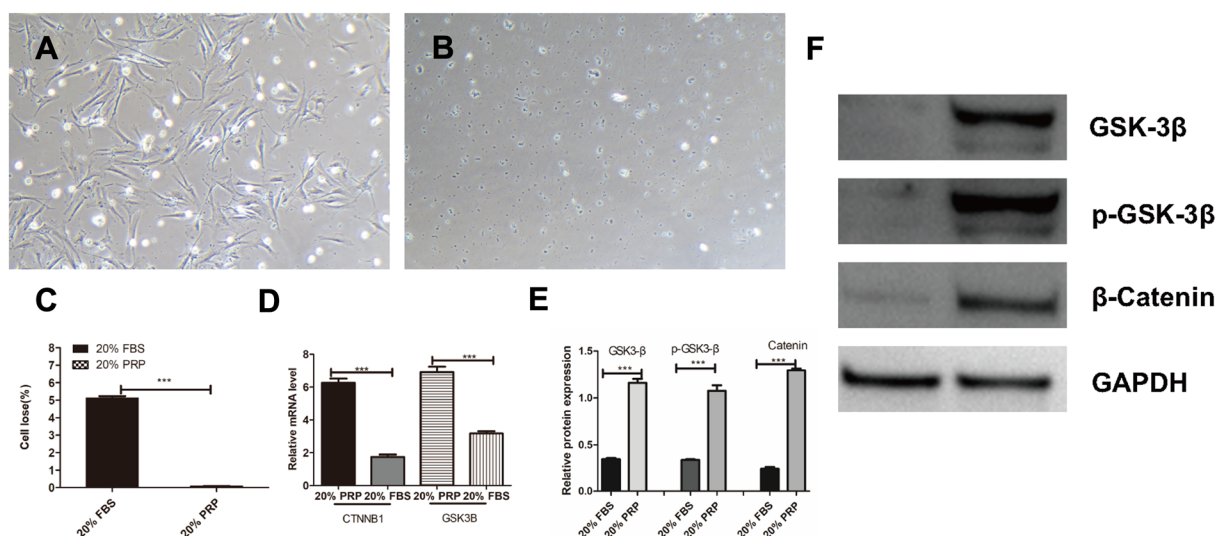


Fig. 4 Cell adhesion assay, cell loss in the control and experimental groups (A–C), qPCR and WB assays for the CTNNB1 and GSK3β genes, and their regulatory proteins GSK-3β and β-catenin (D–F). ***p* < 0.01 vs. the blank group, ****p* < 0.001. All scale bars = 100 μm

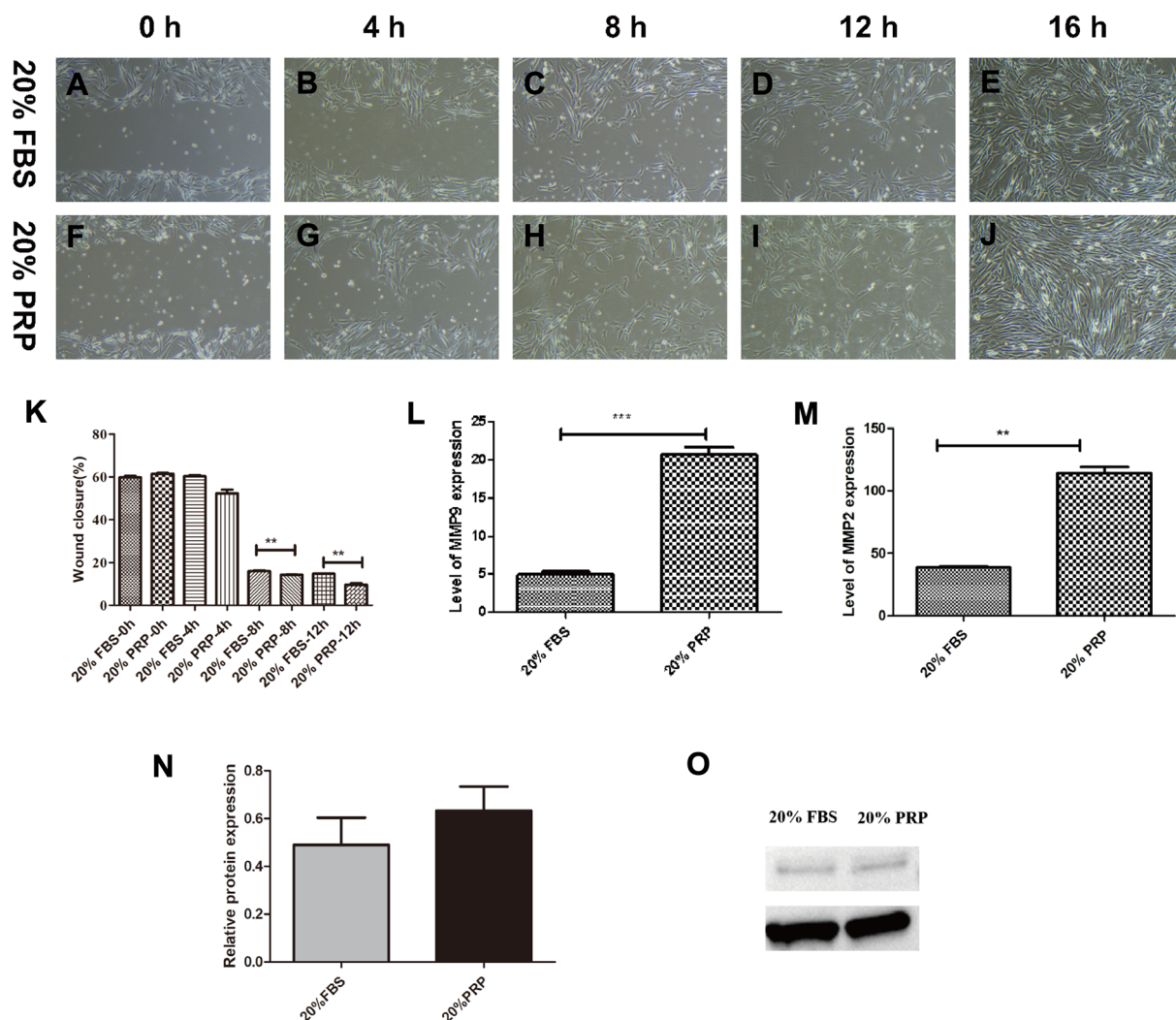


Fig. 5 Graphs of the cell scratch assay and gene expression of MMP2 and MMP9, comparative graphs of the cell migration of the control and experimental groups (A–K), and graphs of the cell migration-related gene expression of MMP-2 and MMP-9 (L, M). Western blot assay to determine the total MMP2 expression (N, O). ** $p < 0.01$ vs. the blank group, *** $p < 0.001$. All scale bars = 100 μm

(Fig. 6B–D). WB results showed that the collagen content of the experimental group was significantly higher than that of the control group (Fig. 6E, F).

Discussion

PRP is widely used in material-assisted applications [24]; however, its application in tissue-engineered vessels is rarely addressed. Does PRP form a connecting bridge between the seed cells of tissue-engineered vessels and the scaffold material, promoting the biological state of adhesion and secretion of SMCs on top of the scaffold material? We do not know. To address this question, we introduced PRP during the inoculation of smooth muscle cells into the scaffold and found that PRP could release the growth factors PDGF-BB and TGF- β continuously

on the scaffold material for up to 30 days by detecting the content of growth factors in the culture medium. We investigated the effect of PRP on smooth muscle cell proliferation and migration by designing different experimental groups, determined the optimal concentration of PRP to use, and studied the adhesion behavior of smooth muscle cells after the addition of PRP and the secretion of collagen under three-dimensional culture conditions.

PRP has been used clinically for decades, and the preparation and distribution of PRP tend to be diverse [25]. The main reason is that PRP is rich in many growth factors [26, 27], among which PDGF-BB and TGF- β are closely related to the biological activity of cells [28, 29]. PDGF and TGF- β were found to significantly promote the proliferative activity of smooth

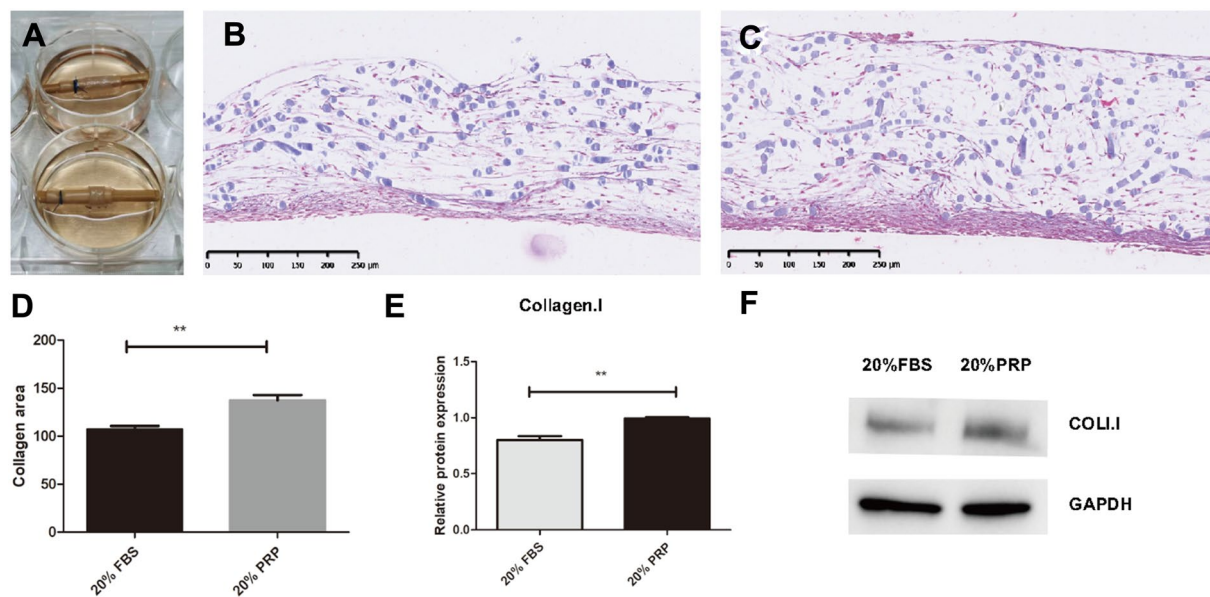


Fig. 6 Three-dimensional culture results and gross plots, 3D culture for both treatments, plots of cultures after 4 weeks of incubation (A), plots of Masson staining and collagen staining for quantitative analysis of cultures (B–D), and WB assay for protein collagen I content and its grayscale value conversion (E, F). ** $p < 0.01$ compared to the blank group, all scale bars = 250 μm

muscle cells [30, 31], and Perrault R et al. showed that PDGF-BB could promote the conversion of smooth muscle cells to a secretory phenotype [32]. PDGF was also shown to promote the migration of smooth muscle cells by regulating the gene expression of MMP2 and MMP9 [33], although PRP contains a large number of growth factors. Although PRP contains a large amount of growth factors, the hydrogel formed after activation of PRP is unstable, and it is difficult to achieve stable release, so many researchers have used it together with other materials, such as PRP combined with sodium alginate for cartilage repair experiments [34], PRP combined with GelMA gel for 3D printing for rabbit cartilage repair experiments [11], or PRP combined with filament proteins using [35]. Although these methods effectively address the problem of PRP hydrogel stability, they are more cumbersome to perform. We added PRP mixed with smooth muscle cells directly to the surface of PGA material, and the electron microscopic results found that the fibrin filaments inside PRP evenly covered and filled the whole PGA fibers and fiber pores, and the adhesion of smooth muscle cells to PGA material because of PRP was not only due the adhesion of smooth muscle cells on PGA fibers but also due to the large number of adhesions between PGA pores. PRP promoted the adhesion of smooth muscle cells inside the PGA material not only by this physical action but also by mechanisms shown by the qPCR results, which

showed that PRP promoted the expression of CTNNB1 and p-GSK-3 β in smooth muscle cells, thus enhancing the adhesion function of smooth muscle cells and promoting the migration of smooth muscle cells through increased gene expression of MMP2 and MMP9. In addition, the results showed that PRP promoted the water uptake of PGA materials.

Collagen I is a major component of the extracellular matrix [36]. To verify that the addition of PRP can ultimately enhance extracellular matrix deposition in vascular tissue engineering, we cultured the experimental and control groups with PRP for 4 weeks and found that the vessels in the experimental group had more collagen deposition, and this result was fully confirmed in the WB experiments. In addition, the technique of repeated freeze–thawing PRP to obtain growth factors is quite mature, and in the future, PRP can be obtained by processing frozen plasma for better application in tissue engineering vessel culture, which is convenient for future clinical applications [15]. Although the experiments showed that the addition of 20% PRP increased the adhesion function and migration of smooth muscle cells on top of PGA material and that the increase in collagen secretion after the addition of PRP was confirmed by three-dimensional culture, the specific mechanism of action remains to be confirmed for future application in tissue-engineered vascular culture.

Conclusion

In this study, we used PRP mixed with smooth muscle cells and added nonwoven PGA material on top of the PRP before it formed a gel using a drop-in method. MMP9 expression was also increased. Three-dimensional culture resulted in more collagen deposition. Our study provides a convenient and effective way to promote good cell adhesion and low cell utilization in tissue-engineered vascular cultures in the future.

Abbreviations

PRP	Plate rich plasma
FBS	Fetal bovine serum
SMC	Smooth muscle cell
ECM	Decellularized extracellular matrix
PGA	Polyglycolic acid
PLLA	Poly-L-lactic acid
PCL	Polycaprolactone
DMEM	Dulbecco's Modified Eagle Medium
TGF- β	Transforming growth factor
PDGF-BB	Platelet-derived growth factor
COL1.1	Collagen type I
CNN	Calponin
SMTN	Smoothelin
MMP2	Matrix metalloproteinase 2
MMP9	Matrix metalloproteinase 9
CTNNB1	Recombinant human catenin beta-1
GSK3 β	Glycogen synthase kinase 3 β
GAPDH	Glyceraldehyde-3-phosphate dehydrogenase

Acknowledgements

None.

Author contributions

YDW contributed to manuscript writing; HJJ, YHW, and QL contributed to the Figs. 2, 3, 4; HHZ and XHS contributed to software analysis; all authors have read and agreed to the published version of the manuscript.

Funding

This work was supported by the Summit Program of The NSFC Incubation Program of GDPH (KY012021150). The authors appreciate all members' support.

Availability of data and materials

Not applicable.

Declarations

Ethics approval and consent to participate

All experiments were conducted in accordance with the ethical regulations of Guangdong Provincial People's Hospital, Guangdong Academy of Medical Sciences, and the ethic number is No.GDREC2019285h. (RI).

Competing interests

The authors report no other competing interests in this work.

Received: 21 August 2023 Accepted: 20 November 2023

Published online: 09 December 2023

References

- Lawson JH, Glickman MH, Ilzecki M, Jakimowicz T, Jaroszynski A, Peden EK, Pilgrim AJ, Prichard HL, Guziewicz M, Przywara S, Szmidt J, Turek J, Witkiewicz W, Zapotoczny N, Zubilewicz T, Niklason LE. Bioengineered human acellular vessels for dialysis access in patients with end-stage renal disease: two phase 2 single-arm trials. *Lancet*. 2016;387(10032):2026–34.
- Pashneh-Tala S, MacNeil S, Claeysens F. The tissue-engineered vascular graft—past, present, and future. *Tissue Eng Part B Rev*. 2016;22(1):68–100.
- Hosseini V, Evrova O, Hoerstrup SP, Vogel V. A simple modification method to obtain anisotropic and porous 3D microfibrillar scaffolds for surgical and biomedical applications. *Small*. 2018;14(4):1702650.
- Liu G, Fu M, Li F, Fu W, Zhao Z, Xia H, Niu Y. Tissue-engineered PLLA/gelatin nanofibrous scaffold promoting the phenotypic expression of epithelial and smooth muscle cells for urethral reconstruction. *Mater Sci Eng C Mater Biol Appl*. 2020;111:110810.
- Li P, Wang Y, Jin X, Dou J, Han X, Wan X, Yuan J, Shen J. Fabrication of PCL/keratin composite scaffolds for vascular tissue engineering with catalytic generation of nitric oxide potential. *J Mater Chem B*. 2020;8(28):6092–9.
- Matsusaki M, Kadowaki K, Adachi E, Sakura T, Yokoyama U, Ishikawa Y, Akashi M. Morphological and histological evaluations of 3D-layered blood vessel constructs prepared by hierarchical cell manipulation. *J Biomater Sci Polym Ed*. 2012;23(1–4):63–79.
- Park IS, Kim SH, Kim YH, Kim IH, Kim SH. A collagen/smooth muscle cell-incorporated elastic scaffold for tissue-engineered vascular grafts. *J Biomater Sci Polym Ed*. 2009;20(11):1645–60.
- Tang Y, Urs S, Boucher J, Bernaiche T, Venkatesh D, Spicer DB, Vary CP, Liaw L. Notch and transforming growth factor-beta (TGFbeta) signaling pathways cooperatively regulate vascular smooth muscle cell differentiation. *J Biol Chem*. 2010;285(23):17556–63.
- Tsuji-Tamura K, Tamura M. Basic fibroblast growth factor uniquely stimulates quiescent vascular smooth muscle cells and induces proliferation and dedifferentiation. *FEBS Lett*. 2022;596(13):1686–99.
- Mijiritsky E, Assaf HD, Peleg O, Shacham M, Cerroni L, Mangani L. Use of PRP, PRF and CGF in periodontal regeneration and facial rejuvenation—a narrative review. *Biology*. 2021;10(4):317.
- Jiang G, Li S, Yu K, He B, Hong J, Xu T, Meng J, Ye C, Chen Y, Shi Z, Feng G, Chen W, Yan S, He Y, Yan R. A 3D-printed PRP-GelMA hydrogel promotes osteochondral regeneration through M2 macrophage polarization in a rabbit model. *Acta Biomater*. 2021;1(128):150–62.
- Qian Z, Wang H, Bai Y, Wang Y, Tao L, Wei Y, Fan Y, Guo X, Liu H. Improving chronic diabetic wound healing through an injectable and self-healing hydrogel with platelet-rich plasma release. *ACS Appl Mater Interfaces*. 2020;12(50):55659–74.
- Andia I, Perez-Valle A, Del Amo C, Maffulli N. Freeze-drying of platelet-rich plasma: the quest for standardization. *Int J Mol Sci*. 2020;21(18):6904.
- Weibrich G, Kleis WK, Hafner G, Hitzler WE. Growth factor levels in platelet-rich plasma and correlations with donor age, sex, and platelet count. *J Craniomaxillofac Surg*. 2002;30(2):97–102.
- Steller D, Herbst N, Pries R, Juhl D, Hakim SG. Impact of incubation method on the release of growth factors in non-Ca2+-activated PRP, Ca2+-activated PRP, PRF and A-PRF. *J Craniomaxillofac Surg*. 2019;47(2):365–72.
- Raicu M, Florea S, Costache G, Popov D, Simionescu M. Clotrimazole inhibits smooth muscle cell proliferation and has a vasodilator effect on resistance arteries. *Fundam Clin Pharmacol*. 2000;14(5):477–85.
- Miano JM, Olson EN. Expression of the smooth muscle cell calponin gene marks the early cardiac and smooth muscle cell lineages during mouse embryogenesis. *J Biol Chem*. 1996;271(12):7095–103.
- Ko HS, Lee S, Lee D, Jho JY. Mechanical properties and bioactivity of poly(lactic acid) composites containing poly(glycolic acid) fiber and hydroxyapatite particles. *Nanomaterials*. 2021;11(1):249.
- Li Y, Wang Z, Liu R. Superparamagnetic α -Fe2O3/Fe3O4 heterogeneous nanoparticles with enhanced biocompatibility. *Nanomaterials*. 2021;11(4):834.
- Park SY, Song WC, Kim B, Oh JW, Park G. Nano-graphene oxide-promoted epithelial-mesenchymal transition of human retinal pigment epithelial cells through regulation of phospholipase D signaling. *Nanomaterials*. 2021;11(10):2546.
- Liu X, Wang L, Ma C, Wang G, Zhang Y, Sun S. Exosomes derived from platelet-rich plasma present a novel potential in alleviating knee osteoarthritis by promoting proliferation and inhibiting apoptosis of chondrocyte via Wnt/ β -catenin signaling pathway. *J Orthop Surg Res*. 2019;14(1):470.
- Huang AH, Niklason LE. Engineering biological-based vascular grafts using a pulsatile bioreactor. *J Vis Exp*. 2011;52:2646.

23. Wan ZH, Li GH, Guo YL, Li WZ, Chen L, Zhang YJ. Amelioration of cavernosal fibrosis and erectile function by lysyl oxidase inhibition in a rat model of cavernous nerve injury. *J Sex Med.* 2018;15(3):304–13.
24. Vocetkova K, Sovkova V, Buzgo M, Lukasova V, Divin R, Rampichova M, Blazek P, Zikmund T, Kaiser J, Karpisek Z, Amler E, Filova E. A simple drug delivery system for platelet-derived bioactive molecules, to improve melanocyte stimulation in Vitiligo treatment. *Nanomaterials.* 2020;10(9):1801.
25. Gentile P, Calabrese C, De Angelis B, Dionisi L, Pizzicannella J, Kothari A, De Fazio D, Garcovich S. Impact of the different preparation methods to obtain autologous non-activated platelet-rich plasma (A-PRP) and activated platelet-rich plasma (AA-PRP) in plastic surgery: wound healing and hair regrowth evaluation. *Int J Mol Sci.* 2020;21(2):431.
26. Mussano F, Genova T, Munaron L, Petrillo S, Erovigni F, Carossa S. Cytokine, chemokine, and growth factor profile of platelet-rich plasma. *Platelets.* 2016;27(5):467–71.
27. Cecerska-Heryc E, Goszka M, Serwin N, Roszak M, Grygorcewicz B, Heryc R, Dolegowska B. Applications of the regenerative capacity of platelets in modern medicine. *Cytokine Growth Factor Rev.* 2022;64:84–94.
28. Zhou S, Ma Y, Yao J, Zhao A, Xie C, Mi Y, Zhang C. TGF- β 1-induced collagen promotes chicken ovarian follicle development via an intercellular cooperative pattern. *Cell Biol Int.* 2021;45(6):1336–48.
29. Loppnow H, Buerke M, Werdan K, Rose-John S. Contribution of vascular cell-derived cytokines to innate and inflammatory pathways in atherosclerosis. *J Cell Mol Med.* 2011;15(3):484–500.
30. Raines EW. PDGF and cardiovascular disease. *Cytokine Growth Factor Rev.* 2004;15(4):237–54.
31. Xie Y, Ostriker AC, Jin Y, Hu H, Sizer AJ, Peng G, Morris AH, Ryu C, Herzog EL, Kyriakides T, Zhao H, Dardik A, Yu J, Hwa J, Martin KA. LMO7 is a negative feedback regulator of transforming growth factor β signaling and fibrosis. *Circulation.* 2019;139(5):679–93.
32. Perrault R, Molnar P, Poole J, Zahradka P. PDGF-BB-mediated activation of CREB in vascular smooth muscle cells alters cell cycling via Rb, FoxO1 and p27kip1. *Exp Cell Res.* 2021;404(1):112612. <https://doi.org/10.1016/j.yexcr.2021.112612>.
33. Higashi Y, Mummidu S, Sukhanov S, Yoshida T, Noda M, Delafontaine P, Chandrasekar B. Minocycline inhibits PDGF-BB-induced human aortic smooth muscle cell proliferation and migration by reversing miR-221- and -222-mediated RECK suppression. *Cell Signal.* 2019;57:10–20.
34. Gao X, Gao L, Groth T, Liu T, He D, Wang M, Gong F, Chu J, Zhao M. Fabrication and properties of an injectable sodium alginate/PRP composite hydrogel as a potential cell carrier for cartilage repair. *J Biomed Mater Res A.* 2019;107(9):2076–87.
35. Li Z, Zhang X, Yuan T, Zhang Y, Luo C, Zhang J, Liu Y, Fan W. Addition of platelet-rich plasma to silk fibroin hydrogel bioprinting for cartilage regeneration. *Tissue Eng Part A.* 2020;26(15–16):886–95.
36. Rebelo SP, Pinto C, Martins TR, Harrer N, Estrada MF, Loza-Alvarez P, Cabeçadas J, Alves PM, Gualda EJ, Sommergruber W, Brito C. 3D-3-culture: a tool to unveil macrophage plasticity in the tumour microenvironment. *Biomaterials.* 2018;163:185–97.

Publisher's Note

Springer Nature remains neutral with regard to jurisdictional claims in published maps and institutional affiliations.

Ready to submit your research? Choose BMC and benefit from:

- fast, convenient online submission
- thorough peer review by experienced researchers in your field
- rapid publication on acceptance
- support for research data, including large and complex data types
- gold Open Access which fosters wider collaboration and increased citations
- maximum visibility for your research: over 100M website views per year

At BMC, research is always in progress.

Learn more biomedcentral.com/submissions

